Journal of Catalysis 284 (2011) 230–235

Contents lists available at SciVerse ScienceDirect

Journal of Catalysis

journal homepage: www.elsevier.com/locate/jcat

Why silver is the unique catalyst for ethylene epoxidation

M.O. Ozbek [a,b], I. Onal [a], R.A. van Santen [b,*]

[a] Chemical Engineering Department, Middle East Technical University, 06531 Ankara, Turkey
[b] Chemical Engineering and Chemistry Department, Eindhoven University of Technology, 5600 MB Eindhoven, The Netherlands

ARTICLE INFO

Article history:
Available online 9 September 2011

Keywords:
DFT
Cu_2O
Ag_2O
Au_2O
Ethylene
Ethylene oxide
Oxide surface

ABSTRACT

The activities of $Cu_2O(001)$, $Ag_2O(001)$, and $Au_2O(001)$ surfaces for direct ethylene epoxidation and alternative paths for EO isomerization are studied. Among these three oxide surfaces, only $Ag_2O(001)$ surface enables direct path without a barrier. Au_2O cannot regenerate surface oxygen, and overall reaction on Cu_2O is endothermic. Furthermore, ring opening of ethylene oxide (EO) and subsequent acetaldehyde (AA) formation on Cu_2O is more favorable than EO desorption. Ethylene adsorption on an oxygen vacancy results in the oxametallacycle (OMC) formation, which causes AA formation and reduces EO selectivity. Cl adsorption removes these surface vacant sites and hence prevents the formation of the OMC intermediate.

© 2011 Elsevier Inc. All rights reserved.

1. Introduction

Silver catalyzed ethylene epoxidation to produce ethylene oxide (EO) is an industrially applied important heterogeneous catalytic process. The EO selectivity of the un-promoted metallic silver lays around 50% [1,2]. However, the industrial catalyst consists of silver particles supported on low surface alumina, with the addition of alkali compounds as promoters. During the process, ppm amounts of chlorine are added to the feed stream as a promoter in the form of chlorinated hydrocarbons, to enhance the EO selectivity. Today, the EO selectivity of the industrial catalyst lies in the range of 90% [3].

Scheme 1 shows the competing parallel (k_1 and k_2) and consecutive (k_4) reactions catalyzed by silver [4]. Formation of acetaldehyde (AA) acts as an intermediate for total combustion [5]. While the parallel reactions (k_1 and k_2) are uniquely catalyzed by Ag, EO isomerization (k_3) predominantly occurs on the alumina support [5,6]. Earlier studies showed that atomic oxygen is the active species for the partial oxidation of ethylene [2,7–9]. Thus the catalyst should be able to dissociate the oxygen molecule, which can be easily achieved on the transition metals as well as by Ag and Cu, but not on Au. On metals that do not activate CH bonds, the surface oxygen has been found to act as a Lewis base that promotes C–H activation [2,10–14]. In the case of ethylene, it has been proposed that this initiates total combustion. Although there are many fundamental studies devoted to understand the Ag epoxidation system, questions like why silver is the unique catalyst, what is the reaction mechanism for high EO selectivity, and what is the role of the Cl promoter are still in debate.

There is a vast number of experimental [15–17] and theoretical [18–20] studies focusing mainly on model systems where silver is essentially metallic under low oxygen pressure regimes. These studies reported that selective (k_1) and non-selective (k_2) parallel reactions proceed through the oxametallacycle (OMC) intermediate [18–25]. OMC forms on the catalyst surface through a well-defined Langmuir–Hinshelwood (L–H) mechanism in a reaction of surface adsorbed atomic oxygen (O_s) with $C_2H_{4(ads)}$. The product selectivity depends on the relative barriers of the product formation (E^a_{EO} and E^a_{AA}) through the decomposition of the OMC intermediate. Studies on the metallic silver surfaces have reported activation barriers for EO and AA formation, which are inconsistent with the high EO selectivity observed in the industrial process. However, the reported non-distinct values of E^a_{EO} and E^a_{AA} would explain the ~50% EO selectivity of the metallic silver.

So far, silver is the only efficient catalyst for ethylene epoxidation. Other transition metal oxidation catalysts give complete combustion [26,27], because of ease of the CH activation. Unlike silver, the literature on the potential of the other metals for ethylene epoxidation is rather scarce. Two computational studies carried out for Cu(111) [25] and Au(111) [23] surfaces with 25% O-coverage reported that the epoxidation reaction proceeds through the OMC intermediate as in the case of metallic silver surfaces. For the Au(111) surface, it was concluded that differences of the activation barriers on Au and Ag are comparable. The main difference between these metallic surfaces relates to the ease of O_2 dissociation. On the other hand, the Cu(111) surface showed a lower activation barrier toward EO formation than that of AA.

---

* Corresponding author at: Chemical Engineering and Chemistry Department, Eindhoven University of Technology, 5600 MB Eindhoven, The Netherlands.

E-mail addresses: m.o.ozbek@tue.nl (M.O. Ozbek), r.a.v.santen@tue.nl (R.A. van Santen).

0021-9517/$ - see front matter © 2011 Elsevier Inc. All rights reserved.
doi:10.1016/j.jcat.2011.08.004

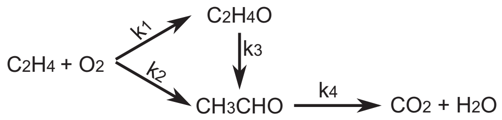

Scheme 1. Molecular mechanism for ethylene epoxidation.

Not withstanding the endothermicity of the reaction of EO formation with respect to pre-adsorbed oxygen on Cu, it was suggested that, in theory, Cu would be a potential interesting candidate for EO catalysis. On the other hand, there is no experimental report of selective epoxidation catalysis of ethylene catalyzed by copper.

Two different studies using gold clusters produced different results. Although a theoretical study [28] concluded that the EO formed through the OMC mechanism with a considerably lower E^a_{EO} than E^a_{AA}, an experimental study [29] showed that Au nanoclusters mainly produced AA.

The concept of subsurface oxygen is not new [2,30–32]. However, the proposal that the oxide surfaces are the active phase for the (partial) oxidation reactions finds recent support [27,33,34]. Furthermore, the presence of subsurface oxygen has been reported to increase catalyst selectivity [35–37] even for the metallic surfaces. For the silver–oxygen systems the local formation of Ag_nO type oxide phases has been suggested [19,35–40], but there is not a definitive model for the overlying oxide structures yet.

In our previous studies [41–43], we have shown that the electrophilic nature of bridging oxygen atoms on the $Ag_2O(001)$ surface makes them very selective for the epoxidation reaction and demonstrated the possibility of a direct epoxidation pathway that proceeds through a low activation energy. This is different from the OMC mechanism that takes place on 3 or 4 coordinated oxygen atoms with nucleophilic nature adsorbed on the metallic Ag surfaces.

Here we will present a comparison of the reactivities of the Cu, Ag, and Au under high oxygen regimes. Since there is no definite model for the surfaces under reaction conditions, the surfaces cut from the well-defined oxide phases Cu_2O, Ag_2O, and Au_2O. Having the same crystal structure, herein computationally studied (001) surfaces contain oxygen atoms in bridge positions. The reaction paths that were previously identified for $Ag_2O(001)$ surface are tested for $Cu_2O(001)$ and $Ag_2O(001)$ surfaces and compared.

2. Computational details

The periodic DFT computations were performed with the VASP package [44,45], using PW basis sets with GGA [46,47]. The cut-off energy used was 500 eV. Necessary dipole corrections due to the asymmetric usage of slabs were included into the computations. All the results presented here were obtained by relaxing the structures until the net force acting on the ions was <0.015 eV/Å. The reaction paths were generated using the climbing image (CI-NEB) method [48]. Spin polarized computations were carried out where necessary and the corresponding energies were reported.

The $M_2O(001)$ surfaces (M: Cu, Ag, Au) were constructed from their respective crystals [13,49] upon optimizing lattice parameters. Each $M_2O(001)$ slab consists of eight atomic layers (for example four Ag_2O layers, 8.5 Å) with a $p(2 \times 2)$ square surface. The supercells were constructed with a minimum vacuum height of 15 Å. In the calculations the bottom layer was kept fixed for all the slabs, where all the remaining atoms were relaxed. The k-points sampling was generated by the Monkhorst Pack procedure with a $(4 \times 4 \times 1)$ mesh for all the slabs. The total energies of gas phase molecules were calculated using single k-point, where the periodic molecules are separated with a minimum of 10 Å vacuum distances.

The vibrational frequencies of adsorbed surface species and transition states were calculated by calculating the Hessian matrix based on a finite difference approach with a step size of 0.02 Å for the displacements of the individual atoms along each Cartesian coordinate. During the frequency calculations, symmetry was excluded explicitly. The frequencies of the surface ions were excluded basing on the frozen phonon approximation.

Zero-point energy (ZPE) corrections were calculated using the harmonic approximation and the positive modes of the vibrational data. ZPE correction was included for both the reactant and the transition state for the reported values of zero-point energy corrected activation energy barriers.

In Fig. 3, the transition states (TS) reported for the direct epoxidation paths could not be verified with frequency calculations; thus, they should be considered as approximate. However, to get the most precise value, all the images along the reaction path were relaxed until the convergence criteria ($F_{net} < 0.015$ eV/Å) was strictly reached. For the geometries corresponding to these peaks, C_2H_4 is not completely surface bound. Thus, frequency calculations do not produce single imaginary frequency as it should be for TS geometry. In these results, two more imaginary frequencies exist for translation and rotation.

3. Results and discussion

3.1. Oxide structures

The formation energies of the bulk oxides from their respective bulk metals are listed in Table 1. The energies are calculated with respect to the reaction:

$$2 \times M_{(bulk)} + 1/2O_{2(gas)} \rightarrow M_{2O(bulk)} \quad (1)$$

As Table 1 shows, the formation of the oxides gets less favorable downward the periodic table. Formation of Au_2O structure is endothermic. However, since it has the same crystal structure as Ag_2O and Cu_2O, the $Au_2O(001)$ surface was evaluated for comparison as well.

A schematic representation of the studied $M_2O(001)$ surfaces is given in Fig. 1. As can be seen, each surface model (i.e., slab) has four O_s in 2-fold bridge positions. Removal of these oxygens creates oxygen vacancies on the surface where metal atoms are exposed to vacuum. Because of the subsurface oxygen atoms, these surface metal atoms are more positively charged ($M^{\delta+}$) compared to their respective metal surfaces. Thus, this oxygen vacancy is a suitable site for O_2 and C_2H_4 adsorption.

3.2. Oxygen adsorption

Fig. 2 compares the adsorption energies of oxygen on the respective oxide surface following the complete removal of the surface oxygen layer (i.e., $4O_s$). When all O_s are removed, the surface shifts to a more metallic state. The adsorption energy of the oxygen on the oxygen-free surface of $Ag_2O(001)$ is very close for the values reported for the metallic surfaces. At 25% coverage, the oxygen adsorption energy is the highest and rapidly converges as the full coverage is achieved. For the metallic surfaces, the

Table 1
Calculated heats of formation for bulk oxides and reference values. The energies are in kJ/mol.

Oxide	ΔH_f	ΔH^0_f
Cu_2O	−134	−169 [14]
Ag_2O	−39	−31 [14]
Au_2O	+21	+22 [13]

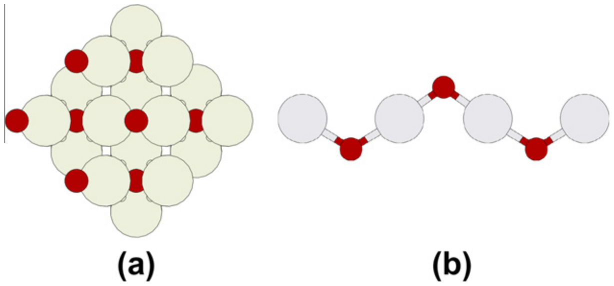

Fig. 1. Schematic representation of the studied $M_2O(001)$ surfaces. (a) Top view and (b) side view of M_2O chain. (M: light gray, O: red or dark gray.) (For interpretation of the references to color in this figure legend, the reader is referred to the web version of this article.)

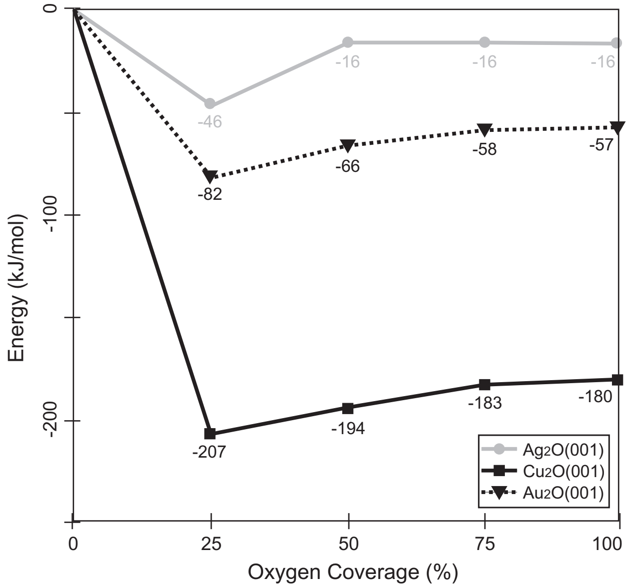

Fig. 2. Oxygen adsorption energies on $M_2O(001)$ surfaces at varying coverage. The energies are calculated with respect to half of the gas phase O_2 energy ($½O_{2(g)}$).

adsorption energies decrease downward the periodic table. The computed oxygen adsorption energies are ~150 kJ/mol for Cu [25], ~50 kJ/mol for Ag [25], and ~10 kJ/mol for Au [23] (111) surfaces. The experimental value for oxygen adsorption to Ag single crystal metal and powders surfaces is around −50 kJ/mol [50,51].

As Table 2 shows, this trend can only be seen for the adsorption energies of the molecular oxygen, however, not for dissociative adsorption. An interesting result is that, the atomic (single O-vacant) and dissociative (two O-vacant) oxygen adsorption on Au_2O surface is more exothermic than adsorption on Ag_2O surface. This finding can be considered to be parallel with a previous study [14], which concluded that the existence of pre-adsorbed atomic oxygen on Au surface favors O_2 dissociation. Furthermore, in case of Au_2O, the larger separation between the metal atoms induces chemical interactions comparable to that of the isolated atoms more than for the metal surface. For instance, atomic covalent bonds to a Au atom tend to be stronger than to Cu or Ag (for e.g., [52]).

The third column of Table 2 lists the adsorption energies of C_2H_4 molecule on an oxygen vacancy (see Fig. 3). When a single O-vacancy is considered, it can be seen that ethylene adsorption will be favored over molecular O_2 adsorption on Ag_2O and Au_2O surfaces. Previously we reported that the reaction of adsorbed ethylene with surface oxygen leads to formation of OMC on the vacant Ag_2O surface and competes with the direct epoxidation. Decomposition of OMC has then also a lower barrier for AA formation (non-selective path) (Fig. 3). The direct selective epoxidation path on Ag_2O has been found to only occur, because OMC formation is prevented. Thus, the absence of surface oxygen vacancies is important to have high EO selectivity. Therefore, rapid generation of the surface oxygens or the site blocking effect of a promoter (i.e., Cl) is essential for the sake of EO selectivity [41].

3.3. Oxygen vacancy and OMC formation

In the case of an O-vacancy, ethylene interacts with the surface metal atoms and adsorbs on this O-vacant site. Fig. 3 compares the elementary reactions that follow ethylene adsorption. Once ad-

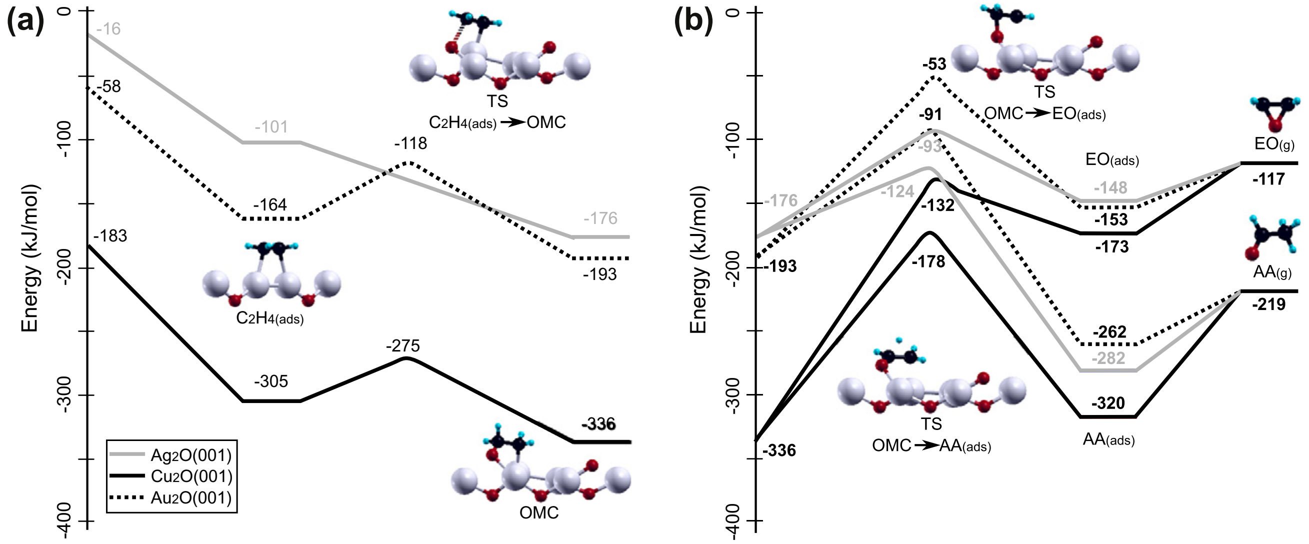

Fig. 3. (a) Relative energies of the formation of the OMC intermediate on an oxygen vacancy, and (b) formation of EO and AA from OMC intermediate. Initial points correspond to oxygen adsorption that shifts the surface coverage to 75%. (M: light gray, O: red or dark gray, C: black, H: cyan or gray.) (For interpretation of the references to color in this figure legend, the reader is referred to the web version of this article.)

Table 2
Adsorption energies (kJ/mol) of O_2 and C_2H_4 on O-vacant surface sites.

	Molecular O_2 adsorption* (–Ag–O–O–Ag–)	Dissociative O_2 adsorption** 2 × (–Ag–O–Ag–)	C_2H_4 adsorption (–Ag–CH_2–CH_2–Ag–)
Cu_2O	−122	−363	−123
Ag_2O	−20	−32	−86
Au_2O	−11	−116	−106

The energies are calculated basing on the reactions:
* $O_{2(g)} + V^* \rightarrow O_{2(ads)}$.
** $O_{2(g)} + 2V^* \rightarrow 2O_s$.

sorbed, the ethylene molecule may interact with a neighboring O_s and form the OMC intermediate. This reaction proceeds through small barriers on Cu_2O and Au_2O; and without a barrier on Ag_2O. Once this OMC intermediate is formed, the reaction may proceed through selective or non-selective channels, as reported for metallic surfaces. However, for all the oxides studied, the formation of AA through the OMC intermediate has lower barrier compared to that of EO. Thus, following the ethylene adsorption, the OMC mechanism predicts preferred formation of AA, which gives a rapid total combustion.

Table 3 compares the activation energies along the OMC path. Starting from OMC intermediate, both forward and backward reactions are considered. Forward reactions produce EO and AA through selective and non-selective channels. In the backward reactions, OMC decomposes to produce ethylene and surface oxygen.

Fig. 3 and Table 3 show that only on Ag_2O and Au_2O, forward reactions are more feasible than backward reaction. On Cu_2O surface, besides being highly stable on the surface, OMC would probably go back to adsorbed ethylene due to lower activation barrier in the backward direction. On Ag_2O and Au_2O, once formed OMC would either produce EO or AA.

3.4. Direct epoxidation

When ethylene is prevented to interact with the surface metal atoms ($M^{\delta+}$) (i.e., no O-vacancy, or site blocker), reaction of the $C_2H_{4(g)}$ and O_s results in the direct formation of EO through a Mars van Krevelen [53] type mechanism as shown in Fig. 4. When $C_2H_{4(g)}$ approaches the surface, it interacts with the O_s to form $EO_{(ads)}$ directly. This is due to the symmetric attack of the electrophilic O_s to the C=C double bond. This reaction channel does not include an intermediate such as OMC. Among the three oxide surfaces considered, only on Ag_2O reaction proceeds without a barrier. Other two surfaces show small barriers for the interaction of $C_2H_{4(g)}$ and O_s. The $Au_2O(001)$ surface appears to have the highest reactivity for EO formation. In essence because of the weaker interaction energy of EO with the single O-vacant Au_2O surface. On the other hand, formation of EO on $Cu_2O(001)$ surface is endothermic. This finding for Cu is in parallel with a previous report for metallic Cu surface [25].

Table 3
Computed and zero-point corrected values for the activation barriers. For the considered forward and backward reactions, OMC is the starting intermediate. Energies are in kJ/mol.

	E^a_{OMC}		E^a_{EO}		E^a_{AA}	
	Comp.	ZPC	Comp.	ZPC	Comp.	ZPC
Cu_2O	63	57	206	201	158	146
Ag_2O	75*	75*	83	82	53	46
Au_2O	140	133	75	68	102	89

* E^a_{OMC} for $Ag_2O(001)$ corresponds to the energy required to desorb ethylene from the surface. See Fig. 4.

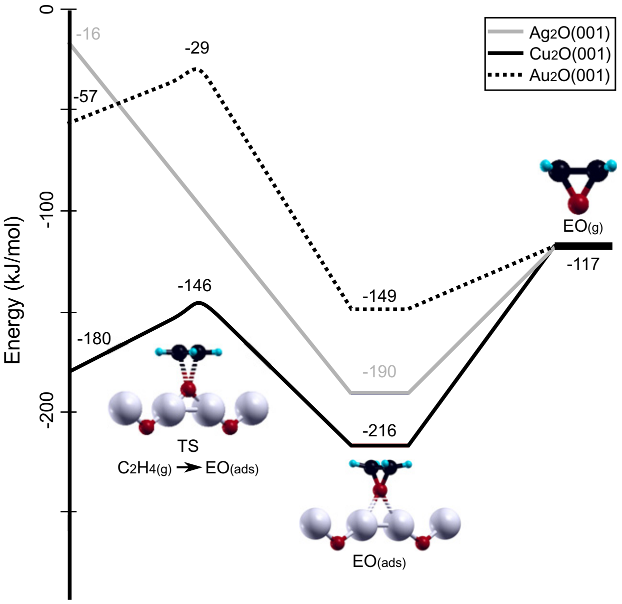

Fig. 4. Relative energies of direct epoxidation paths on $M_2O(001)$ surfaces. Initial points correspond to the oxygen adsorption energies on a vacant surface site that saturates the surface. (M: light gray, O: red or dark gray, C: black, H: cyan or gray.) (For interpretation of the references to color in this figure legend, the reader is referred to the web version of this article.)

When the OMC mechanism, as reported for metallic surfaces, and the direct mechanism on $Ag_2O(001)$ surface are compared, it can be seen that the activation energies of the rate controlling steps in both reaction mechanisms (i.e., OMC vs. direct mechanism) are similar and agree with experimentally reported values that are around 70 kJ/mol [54,55]. However, the corresponding reaction steps are different (i.e., OMC activation vs. EO desorption). The rate controlling step of the direct mechanism is the EO desorption. The order of EO desorption energies follow the relative stability of the oxides (or the strength of oxygen binding). Desorption of the epoxide to be rate limiting is consistent with the observed low reaction order in ethylene but a high reaction order in oxygen [56]. Furthermore, the reported [57] increase of the EO selectivity with the increasing oxygen coverage is also consistent with the preference for EO formation on an oxidized Ag surface in this manner.

3.5. EO isomerization

In order to successfully obtain EO as the product, it has to desorb from the surface without further reaction. Upon its formation on the oxide surface, three possible follow-up paths are considered. These are, (i) desorption, (ii) ring opening, and (iii) isomerization to AA. The relative energies of these paths are compared in Fig. 5.

The horizontal line in Fig. 5 (−117 kJ/mol) shows the energy level of desorbed EO. The left part of the figure shows the formation

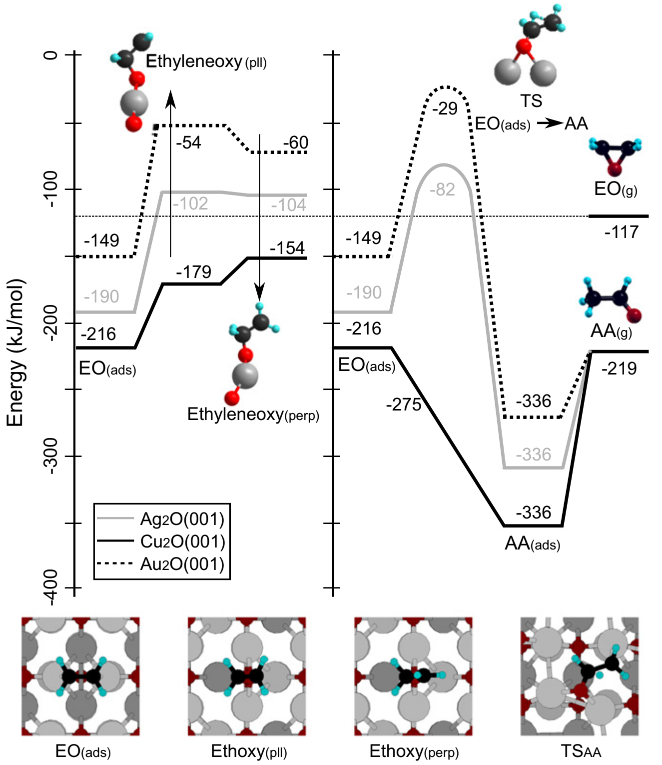

Fig. 5. Comparison of the energy changes of reaction paths following EO formation. Adsorbed EO may (i) desorb, (ii) isomerize to ethyleneoxy intermediate, or (iii) isomerize to AA.

of ethyleneoxy intermediate through ring opening of adsorbed EO. Starting from $EO_{(ads)}$, when one of the O–C bonds activate, first ethyleneoxy$_{(pll)}$ intermediate forms where the H atoms of the free CH_2 group stays parallel to the surface plane, and then they become perpendicular to the surface with the rotation. This kind of a ring opening and rotation of CH_2 group explains the cis–trans isomerization observed in experimental studies [58,59]. Ethyleneoxy$_{(perp)}$ intermediate would go back to $EO_{(ads)}$ following the same path backward. The similar energies required for EO isomerization and desorption on $Ag_2O(001)$ surface can explain the equal distributions of cis and trans isomers as observed in experimental studies.

The right part of Fig. 5 shows the EO isomerization to AA starting from $EO_{(ads)}$. On Ag_2O and Au_2O surfaces, this isomerization goes through respective activation barriers, which are substantially higher than the energy required for EO desorption. This indicates that EO desorption will be the preferred path instead of AA formation. On Cu_2O, however, isomerization of EO to AA is quite exothermic and does not have a barrier. The strong Cu–O_s interaction causes an easy activation of the C–O and/or C–H bond of the $EO_{(ads)}$. Thus, although direct formation of adsorbed EO on Cu_2O surface is more exothermic compared to other surfaces, the overall reaction is non-selective because of rapid EO isomerization to AA. Also, giving the most exothermic EO formation, Cu_2O surface has the highest EO desorption energy.

4. Conclusions

This study aims to computationally analyze the epoxidation selectivity of ethylene on highly oxygenated surfaces of transition metals Cu, Ag, and Au. Concerning ethylene epoxidation, highly oxidized catalyst surface has been suggested to be selective; however, a conclusive model of the Ag surface at the epoxidation conditions does not exist. Thus, in this study the reactivities of well-defined $Cu_2O(001)$, $Ag_2O(001)$, and $Au_2O(001)$ oxide surfaces were explored toward ethylene epoxidation. The relative stabilities and the oxygen binding energies of these compounds decrease downward the periodic table. The Au_2O structure is not a stable oxide structure, but having the same crystal structure with Ag_2O and Cu_2O, its reactivity has been used for comparison. For the three $M_2O(001)$ surfaces studied, a direct epoxidation channel has been found to exist with a low or no barrier.

An interesting point is the different trends observed in the reactivities of the metallic surfaces with monolayer oxygen coverage, and the studied oxide surfaces. The metallic Cu surface where atomic oxygen lies in the 3-fold sites has been shown computationally to be more selective for EO than Ag [25]. On the other hand, the oxide surface of Ag with oxygen in 2-fold bridge positions shows a unique high selectivity for EO, as an epoxidation catalyst, whereas we find here that the Cu_2O surface has a very low selectivity toward EO formation. The preferred use of Ag versus Cu in the catalytic reaction relates to differences in reactivity of the catalysts in the oxidic state rather than the metallic state.

Non-selective AA formation is found to compete with EO formation only on the Cu_2O surface. This is essentially due to the relatively weak O–C bond interaction and the high desorption energy of EO.

The OMC intermediate forms exothermically on O-vacant surface sites of all studied oxides. For all three surfaces studied, the barrier for AA formation through the OMC intermediate was found to be lower than that of EO formation. The $Cu_2O(001)$ surface gave the most exothermic OMC formation and the highest consequent EO and AA barriers. The $Ag_2O(001)$ and $Au_2O(001)$ surfaces show more moderate energy values along the OMC mechanism.

Au_2O is not a stable structure and Cu_2O does not favor the EO formation. The intermediate value of Ag_2O's stability and its oxygen bond strength placed between Au_2O and Cu_2O relate the uniqueness of the silver catalyst for ethylene epoxidation. The interaction of $Ag_2O(001)$ surface with molecular oxygen is strong enough to re-oxidize the Ag surface to the oxide, on the other hand weak enough to prevent the ring opening of EO as well as to prevent the activation of the CH bonds.

An additional prerequisite for high selectivity is the absence of O-vacancies, where the non-selective reaction takes places through OMC intermediate. Most likely this is the moderating role of Cl that is added to the catalyst as promoter. This is subject to our ongoing investigations.

Acknowledgments

This work was supported by NWO-NCF and SARA for the computation time on Huygens computer system with Project No. SH-074-09 and was supported in part by TÜBİTAK through TR-Grid e-Infrastructure Project.

References

[1] P. Christopher, S. Linic, Engineering selectivity in heterogeneous catalysis: Ag nanowires as selective ethylene epoxidation catalysts, J. Am. Chem. Soc. 130 (2008) 11264–11265.
[2] R.A. Van Santen, H.P.C.E. Kuipers, The mechanism of ethylene epoxidation, in: H.P.D.D. Eley, B.W. Paul (Eds.), Advances in Catalysis, Academic Press, 1987. pp. 265–321.
[3] SHELL, Ethylene oxide/ethylene glycol (EO/EG) processes, in: SHELL, 2010.
[4] H.H. Voge, C.R. Adams, Catalytic oxidation of olefins, in: H.P.D.D. Eley, B.W. Paul (Eds.), Advances in Catalysis, Academic Press, 1967. pp. 151–221.
[5] D.A. Bulushev, E.A. Paukshtis, Y.N. Nogin, B.S. Bal'zhinimaev, Transient response and infrared studies of ethylene oxide reactions on silver catalysts and supports, Appl. Catal. A: Gen. 123 (1995) 301–322.
[6] S.N. Goncharova, E.A. Paukshtis, B.S. Bal'zhinimaev, Size effects in ethylene oxidation on silver catalysts. Influence of support and Cs promoter, Appl. Catal. A: Gen. 126 (1995) 67–84.
[7] C.T. Campbell, Chlorine promoters in selective ethylene epoxidation over Ag(111): a comparison with Ag(110), J. Catal. 99 (1986) 28–38.

[8] R.B. Grant, R.M. Lambert, Mechanism of the silver-catalysed heterogeneous epoxidation of ethylene, J. Chem. Soc., Chem. Commun. (1983) 662–663.

[9] R.B. Grant, R.M. Lambert, A single crystal study of the silver-catalysed selective oxidation and total oxidation of ethylene, J. Catal. 92 (1985) 364–375.

[10] E.M. Stuve, R.J. Madix, Bonding and dehydrogenation of ethylene on palladium metal. Vibrational spectra and temperature-programmed reaction studies on palladium (1 0 0), J. Phys. Chem. 89 (1985) 105–112.

[11] C.M. Friend, X. Xu, Reactions on transition-metal surfaces, Annu. Rev. Phys. Chem. 42 (1991) 251–278.

[12] M. Frank, M. Baumer, R. Kuhnemuth, H.-J. Freund, Adsorption and reaction of ethene on oxide-supported Pd, Rh, and Ir particles, in: AVS, Boston, MA (USA), 2001, pp. 1497–1501.

[13] H. Shi, R. Asahi, C. Stampfl, Properties of the gold oxides Au_2O_3 and Au_2O: first-principles investigation, Phys. Rev. B 75 (2007) 205125.

[14] Handbook of Chemistry & Physics Online, in: CRC, 2011.

[15] A. Klust, R.J. Madix, Selectivity limitations in the heterogeneous epoxidation of olefins: branching reactions of the oxametallacycle intermediate in the partial oxidation of styrene, J. Am. Chem. Soc. 128 (2006) 1034–1035.

[16] F.J. Williams, D.P.C. Bird, A. Palermo, A.K. Santra, R.M. Lambert, Mechanism, selectivity promotion, and new ultraselective pathways in Ag-catalyzed heterogeneous epoxidation, J. Am. Chem. Soc. 126 (2004) 8509–8514.

[17] J.R. Monnier, J.L. Stavinoha, G.W. Hartley, Effects of chlorine and chlorine dynamics during silver-catalyzed epoxidation of butadiene, J. Catal. 226 (2004) 321–333.

[18] S. Linic, M.A. Barteau, Control of ethylene epoxidation selectivity by surface oxametallacycles, J. Am. Chem. Soc. 125 (2003) 4034–4035.

[19] M.-L. Bocquet, A. Michaelides, D. Loffreda, P. Sautet, A. Alavi, D.A. King, New insights into ethene epoxidation on two oxidized Ag{1 1 1} surfaces, J. Am. Chem. Soc. 125 (2003) 5620–5621.

[20] M.-L. Bocquet, D. Loffreda, Ethene epoxidation selectivity inhibited by twisted oxametallacycle: a DFT study on Ag surface-oxide, J. Am. Chem. Soc. 127 (2005) 17207–17215.

[21] S. Linic, M.A. Barteau, Formation of a stable surface oxametallacycle that produces ethylene oxide, J. Am. Chem. Soc. 124 (2001) 310–317.

[22] S. Linic, M.A. Barteau, Construction of a reaction coordinate and a microkinetic model for ethylene epoxidation on silver from DFT calculations and surface science experiments, J. Catal. 214 (2003) 200–212.

[23] D. Torres, F. Illas, On the performance of Au(1 1 1) for ethylene epoxidation: a density functional study, J. Phys. Chem. B 110 (2006) 13310–13313.

[24] D. Torres, N. Lopez, F. Illas, A theoretical study of coverage effects for ethylene epoxidation on Cu(1 1 1) under low oxygen pressure, J. Catal. 243 (2006) 404–409.

[25] D. Torres, N. Lopez, F. Illas, R.M. Lambert, Why copper is intrinsically more selective than silver in alkene epoxidation: ethylene oxidation on Cu(1 1 1) versus Ag(1 1 1), J. Am. Chem. Soc. 127 (2005) 10774–10775.

[26] M. Mavrikakis, D.J. Doren, M.A. Barteau, Density functional theory calculations for simple oxametallacycles: trends across the periodic table, J. Phys. Chem. B 102 (1998) 394–399.

[27] K. Reuter, M. Scheffler, Oxide formation at the surface of late 4D transition metals: insights from first-principles atomistic thermodynamics, Appl. Phys. A: Mater. Sci. Process. 78 (2004) 793–798.

[28] H.-T. Chen, J.-G. Chang, S.-P. Ju, H.-L. Chen, Ethylene epoxidation on a Au nanoparticle versus a Au(1 1 1) surface: a DFT study, J. Phys. Chem. Lett. 1 (2010) 739–742.

[29] J. Sebera, H. Hoffmannová, P. Krtil, Z. Samec, S. Zális, Electrochemical and density functional studies of the catalytic ethylene oxidation on nanostructured Au electrodes, Catal. Today 158 (2010) 29–34.

[30] C. Backx, J. Moolhuysen, P. Geenen, R.A. van Santen, Reactivity of oxygen adsorbed on silver powder in the epoxidation of ethylene, J. Catal. 72 (1981) 364–368.

[31] P.J. Van den Hoek, E.J. Baerends, R.A. Van Santen, Ethylene epoxidation on silver(1 1 0): the role of subsurface oxygen, J. Phys. Chem. 93 (1989) 6469–6475.

[32] R.A. van Santen, C.P.M. de Groot, The mechanism of ethylene epoxidation, J. Catal. 98 (1986) 530–539.

[33] M. Gajdos, A. Eichler, J. Hafner, Ab initio density functional study of O on the Ag(0 0 1) surface, Surf. Sci. 531 (2003) 272–286.

[34] P. Frondelius, H. Häkkinen, K. Honkala, Formation of gold(I) edge oxide at flat gold nanoclusters on an ultrathin MgO film under ambient conditions, Angew. Chem. Int. Ed. 49 (2010) 7913–7916.

[35] L.S. Kibis, A.I. Stadnichenko, E.M. Pajetnov, S.V. Koscheev, V.I. Zaykovskii, A.I. Boronin, The investigation of oxidized silver nanoparticles prepared by thermal evaporation and radio-frequency sputtering of metallic silver under oxygen, Appl. Surf. Sci. 257 (2010) 404–413.

[36] H.-Y. Su, Z. Zeng, X.-H. Bao, W.-X. Li, First-principles study of carbon monoxide oxidation on Ag(1 1 1) in presence of subsurface oxygen and stepped Ag(2 2 1), J. Phys. Chem. C 113 (2009) 8266–8272.

[37] Y. Xu, J. Greeley, M. Mavrikakis, Effect of subsurface oxygen on the reactivity of the Ag(1 1 1) surface, J. Am. Chem. Soc. 127 (2005) 12823–12827.

[38] J. Schnadt, A. Michaelides, J. Knudsen, R.T. Vang, K. Reuter, Aelig, E. Gsgaard, M. Scheffler, F. Besenbacher, Revisiting the structure of the $p(4 \times 4)$ surface oxide on Ag(1 1 1), Phys. Rev. Lett. 96 (2006) 146101.

[39] M. Schmid, A. Reicho, A. Stierle, I. Costina, J. Klikovits, P. Kostelnik, O. Dubay, G. Kresse, J. Gustafson, E. Lundgren, J.N. Andersen, H. Dosch, P. Varga, Structure of Ag(1 1 1)–$p(4 \times 4)$–O: no silver oxide, Phys. Rev. Lett. 96 (2006) 146102.

[40] A. Michaelides, K. Reuter, M. Scheffler, When seeing is not believing: oxygen on Ag(1 1 1), a simple adsorption system?, J Vac. Sci. Technol. A: Vac., Surf., Films 23 (2005) 1487–1497.

[41] M.O. Özbek, I. Önal, R.A.v. Santen, Ethylene epoxidation catalyzed by chlorine promoted silver oxide, J. Phys.: Condens. Matter, in press.

[42] M.O. Özbek, I. Önal, R.A. van Santen, Ethylene epoxidation catalyzed by silver oxide, ChemCatChem 3 (2011) 150–153.

[43] M. Fellah, R. van Santen, I. Onal, Epoxidation of ethylene by silver oxide (Ag_2O) cluster: a density functional theory study, Catal. Lett. 141 (2011) 762–771.

[44] G. Kresse, J. Furthmüller, Efficiency of ab-initio total energy calculations for metals and semiconductors using a plane-wave basis set, Comput. Mater. Sci. 6 (1996) 15–50.

[45] G. Kresse, J. Hafner, Ab initio molecular-dynamics simulation of the liquid-metal–amorphous-semiconductor transition in germanium, Phys. Rev. B 49 (1994) 14251.

[46] P.E. Blöchl, Projector augmented-wave method, Physical Review B, 50 (1994) 17953.

[47] J.P. Perdew, J.A. Chevary, S.H. Vosko, K.A. Jackson, M.R. Pederson, D.J. Singh, C. Fiolhais, Erratum: atoms, molecules, solids, and surfaces: applications of the generalized gradient approximation for exchange and correlation, Phys. Rev. B 48 (1993) 4978.

[48] G. Henkelman, H. Jonsson, Improved tangent estimate in the nudged elastic band method for finding minimum energy paths and saddle points, J. Chem. Phys. 113 (2000) 9978–9985.

[49] T. Suzuki, X-ray study on the binding properties of Cu_2O and Ag_2O crystals, J. Phys. Soc. Jpn. 15 (2018).

[50] C.T. Campbell, Atomic and molecular oxygen adsorption on Ag(1 1 1), Surf. Sci. 157 (1985) 43–60.

[51] M. Dean, M. Bowker, Adsorption studies on catalysts under UHV/HV conditions: I. Oxygen adsorption on alumina supported silver, Appl. Surf. Sci. 35 (1988) 27–40.

[52] L. Barrio, P. Liu, J.A. Rodriguez, J.M. Campos-Martin, J.L.G. Fierro, Effects of hydrogen on the reactivity of O_2 toward gold nanoparticles and surfaces, J. Phys. Chem. C 111 (2007) 19001–19008.

[53] P. Mars, D.W. van Krevelen, Oxidations carried out by means of vanadium oxide catalysts, Chem. Eng. Sci. 3 (1954) 41–59.

[54] A.L. Larrabee, R.L. Kuczkowski, The oxidation of ethylene-1,2-d2 over a silver catalyst studied by microwave spectroscopy, J. Catal. 52 (1978) 72–80.

[55] H. Kanoh, T. Nishimura, A. Ayame, Supported silver catalysts for the oxidation of ethylene: the effects of thermal treatment of alumina as catalyst support, J. Catal. 57 (1979) 372–379.

[56] P.D. Klugherz, P. Harriott, Kinetics of ethylene oxidation on a supported silver catalyst, AIChE J. 17 (1971) 856–866.

[57] L.M. Akella, H.H. Lee, Selectivity characterization of ethylene oxidation reactions: oxygen chemisorption, J. Catal. 86 (1984) 465–472.

[58] N.W. Cant, W.K. Hall, Catalytic oxidation: VI. Oxidation of labeled olefins over silver, J. Catal. 52 (1978) 81–94.

[59] W.F. Richey, Stereochemistry of the silver-catalyzed epoxidation of olefins, J. Phys. Chem. 76 (1972) 213–216.